Research Article

Seyyed Mohammad Ebrahimi, Javad Safaei-Ghomi*, and Mohammaed Abdulridha Mutashar

HPA-ZSM-5 nanocomposite as high-performance catalyst for the synthesis of indenopyrazolones

https://doi.org/10.1515/mgmc-2022-0003
received March 21, 2021; accepted February 22, 2022

Abstract: tHPA-ZSM-5 nanocomposites as a superior catalyst have been applied for the synthesis of indenopyrazolones through a three-component reaction of phenylhydrazine, benzaldehydes, and indan-1,2,3-trione at room temperature in acetonitrile. The zeolite catalyst has been characterized by X-ray diffraction, field emission scanning electronic microscopes, Fourier transform infrared, energy-dispersive spectroscopy, thermogravimetric analysis, and N_2-adsorption analysis. The various aromatic aldehydes can be utilized in this method. These results showed that aromatic aldehydes with electron-withdrawing groups reacted faster than aldehydes with electron-releasing groups. Experimental simplicity, excellent yields in short reaction times, reusability of the catalyst, and low catalyst loading are some of the substantial features of this method.

Keywords: catalyst, indenopyrazolones, HPA-ZSM, one-pot, zeolite

1 Introduction

Pyrazolones show anticancer (Saidachary et al., 2014), antimicrobial (Indrasena et al., 2014), antianalgesic (Khalil et al., 2014), antioxidant (Mazimba et al., 2014), antibacterial (Sivakumar et al., 2014), anti-diabetic (Mor and Sindhu, 2020), antifungal (Mor et al., 2017), antitumor (Rostom, 2006), and anticonvulsant (Ahsan et al., 2013) activities. Indenofused heterocycles have received considerable attention from synthetic chemists and medicinal professionals in recent years (Kaur et al., 2020; Singh et al., 2005, Singh, 2016). These properties make pyrazolones substantial objectives in organic synthesis. The past reports on the synthesis of pyrazolones have mentioned such catalysts as CH_3COOH (Mor et al., 2019), $[HMIM]HSO_4$ (Zang et al., 2011), 3-aminopropylated silica gel (Sobhani et al., 2012), sodium dodecyl sulfate (SDS) (Wang et al., 2005), silica-bonded S-sulfonic acid (Niknam et al., 2010), and Ce/SiO_2 composites (Akondi et al., 2016). Each of these catalysts may have its own benefits but also suffer apparent disadvantages including high reaction times, low efficiency, unwanted reaction conditions, and the use of non-green catalysts. Therefore, to avoid these limitations, the discovery of an effective method for the synthesis of pyrazolones is still favored. The facility of accomplishment multicomponent reactions with a recyclable catalyst could advance the efficiency of organic reactions (Alirezvani et al., 2019; Davoodi et al., 2019). Heteropolyacids (HPAs) have polyoxometalate inorganic cages, which may adopt the Keggin structure with the common formula $H_3MX_{12}O_{40}$, where X is the heteroatom and M is the central atom. Generally, M can be either Si or P, and X = Mo or W (Timofeeva, 2003). Immobilization of HPAs on silica structures as support results in more stability and increased catalytic activity (Molnár et al., 1999; Sofia et al., 2009). HPAs have been heterogenized using immobilization of HPAs on zirconium dioxide (Sunita et al., 2008), titanium dioxide (Waghmare et al., 2008), silica (Izumi et al., 1999; Safaei-Ghomi et al., 2020), zeolite (Mukai et al., 2003), and SBA-15 or MCM-41 (Bordoloi et al., 2007; Wang and Zhu, 2004). In this context, among different solid supports, nanocrystalline ZSM-5 zeolite is most preferred because of its many advantageous properties such as high surface area with different active sites, small pore sizes, short diffusion path, excellent chemical and thermal stability, and good accessibility (Liu et al., 2015; Su et al., 2020; Takmil et al., 2021; Xue et al., 2012). Ideally, utilizing environmental and green catalysts which can be easily recycled at the end of reactions has obtained great attention in recent years

* **Corresponding author: Javad Safaei-Ghomi,** Department of Organic Chemistry, Faculty of Chemistry, University of Kashan, P.O. Box 87317-51167, Kashan, Iran, e-mail: safaei@kashanu.ac.ir
Seyyed Mohammad Ebrahimi: Department of Organic Chemistry, Faculty of Chemistry, University of Kashan, P.O. Box 87317-51167, Kashan, Iran
Mohammaed Abdulridha Mutashar: Department of Inorganic Chemistry, Faculty of Chemistry, University of Kashan, Kashan, 51167, Iran

(Ghanbari et al., 2016; Gholamian et al., 2013). Heterogeneous catalysts are defined as solids or mixtures of solids that accelerate the chemical reaction without themselves undergoing changes (Dai et al., 2021; Karimi-Maleh et al., 2020; Keyikoglu et al., 2022; Orooji et al., 2021; Taherian et al., 2022). Nanostructures exhibit good catalytic activity due to their large surface area and active sites which are mainly responsible for their catalytic activity (Masoumi et al., 2016; Nabiyouni et al., 2015). In the current study, we investigated an easy way for the synthesis of indenopyrazolones through three-component reactions of phenylhydrazine, benzaldehydes, and indan-1,2,3-trione using HPA-ZSM-5 at room temperature in acetonitrile (Scheme 1).

2 Results and discussion

The prepared catalyst was characterized by spectral techniques including X-ray diffraction (XRD), field emission scanning electronic microscopes (FE-SEM), Fourier transform infrared (FT-IR), energy-dispersive spectroscopy (EDX), thermogravimetric analysis (TGA), and N_2-adsorption analysis, and BET analyses.

FT-IR studies on zeolite ZSM-5 and its immobilized catalysts were carried out (Figure 1). The unmodified product has bands at the following wavenumbers (cm^{-1}): 548 (δSi–O–Si), 796 (νsSi–O–Si), 1,096 (νasSi–O–Si), 1,630 (adsorbed H_2O), and 3,448 (νOH). The 796 band was shifted in the phosphomolybdic acids-modified sample to 787 cm^{-1} that is the result of overlapping with bands δ Mo–O–Mo (754 cm^{-1}) (Javidi et al., 2014). The band of silanol groups shifted in the case of PMA-containing sample only. In addition, a new strong band at 962 cm^{-1} appeared in the spectra of modified ZSM-5. This band is typical for Keggin's structure of HPAs and corresponds to vasMo–O–Mo or vasW–O–W vibrations (Amini et al., 2006).

FE-SEM images of ZSM-5 and its immobilized catalyst are provided in Figure 2. After the immobilization, the surfaces of the catalyst were covered with a white translucent

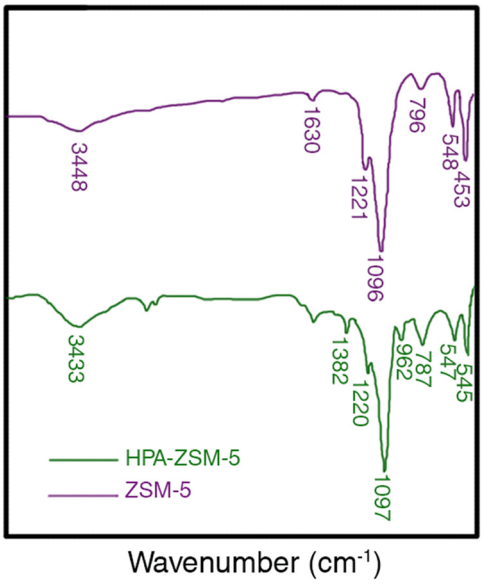

Figure 1: Fourier-transform infrared spectroscopy spectra of ZSM-5 and HPA-ZSM-5.

substance, and the surfaces became smoother. The particles became larger in size, and their profiles became clearer, indicating that HPA was immobilized on the surface of ZSM-5. The evaluation of the used catalyst structure by FE-SEM evidence that the morphology of the catalyst remained unchanged after the fifth cycle (Figure 2b and c).

EDX analysis (Figure 3) of the catalyst showed the presence of Al, P, O, Si, and Mo elements confirming the formation of the catalytic system as visualized. Elemental mapping images (Figure 3) of the catalyst showed uniform distribution of the elements P and Mo in the desired catalytic system.

The XRD patterns of ZSM-5 and its immobilized catalyst are shown in Figure 4. In pattern (a), the peaks of high intensity at 23.4°, 24.1°, and 24.6° are the characteristic diffraction peaks of ZSM-5, indicating good crystallinity of our synthesized ZSM-5 (JCPDS = 44-0003). Compared with the ZSM-5 pattern, the HPA-ZSM-5 pattern exhibits all the diffraction peaks of ZSM-5, and the shape

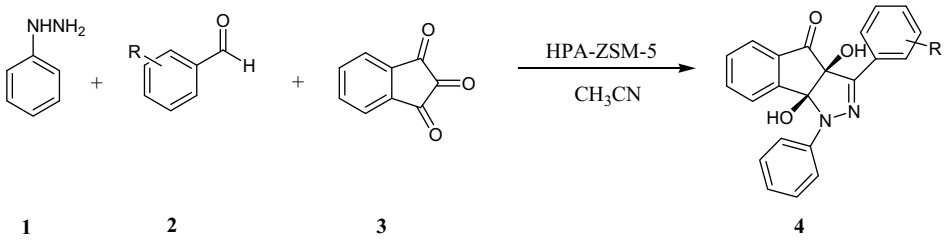

Scheme 1: Synthesis of indenopyrazolones.

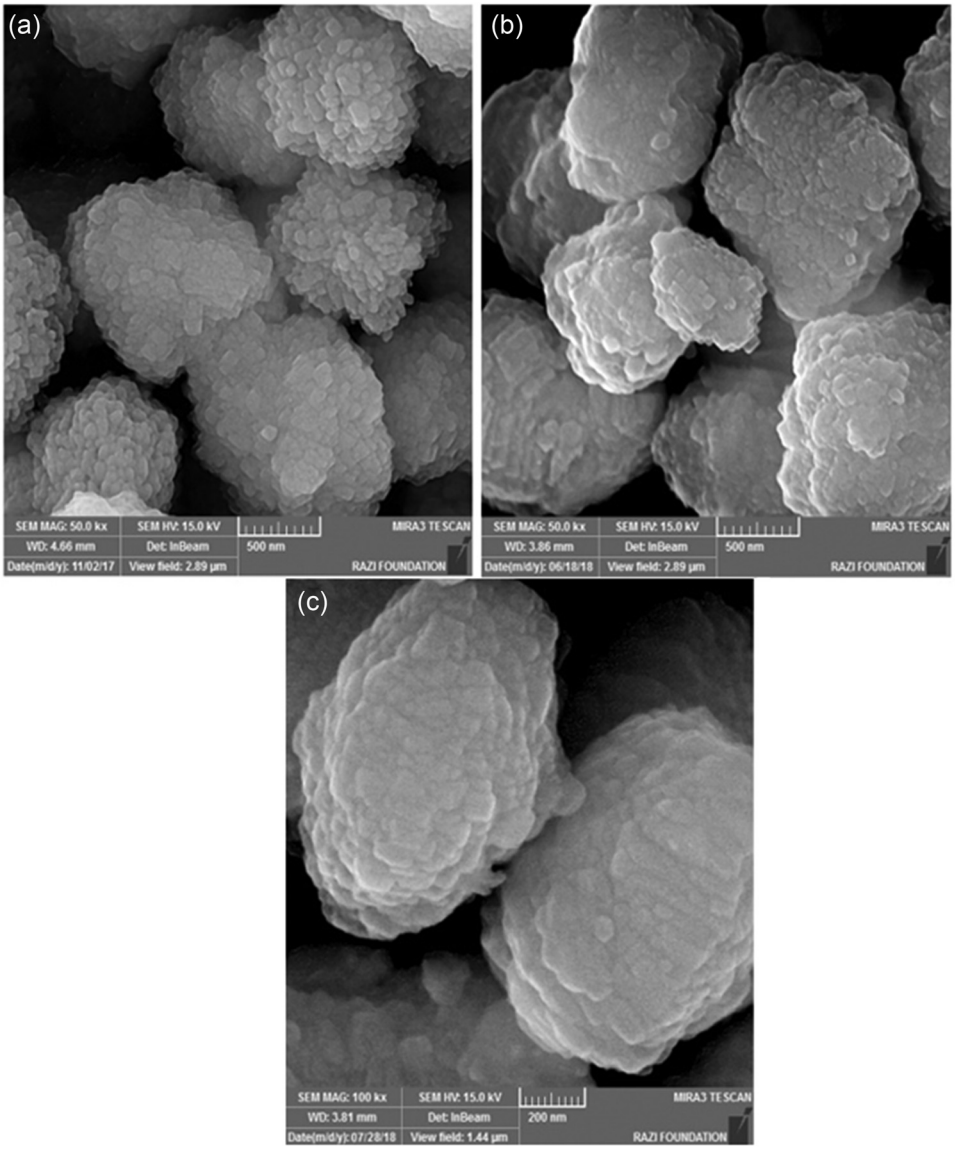

Figure 2: FE-SEM images of: (a) ZSM-5, (b) HPA-ZSM-5, and (c) the used HPA-ZSM-5.

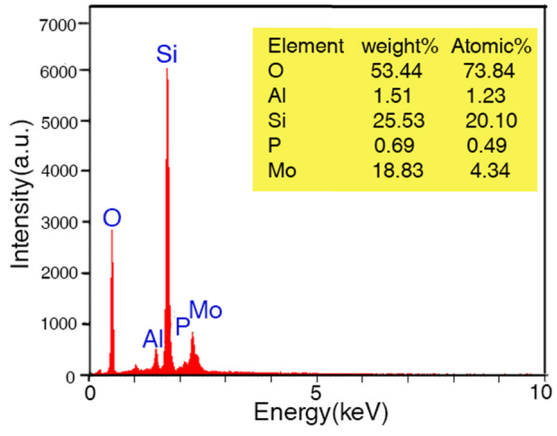

Figure 3: EDS of HPA-ZSM-5.

and intensity of the diffraction peaks have negligible changes, indicating that the prepared catalysts maintained the good crystallinity of ZSM-5 after the immobilization of the HPA onto ZSM-5.

N_2-sorption isotherms at 77 K of ZSM-5 and HPA-ZSM-5 are indicated in Figure 5. As shown in Figure 5, all the isotherms exhibited a typical type IV isotherm with an H1 hysteresis loop starting from $P/P_0 = 0.5$. The results presented that the BET-specific surface area of ZSM-5 increased from 170 to 240 $m^2 \cdot g^{-1}$ after modification with HPA.

Thermogravimetric analysis (TGA) evaluates the thermal stability of HPA-ZSM-5 (Figure 6). A 3% decrease in weight between 100°C and 250°C is because of losing absorbed

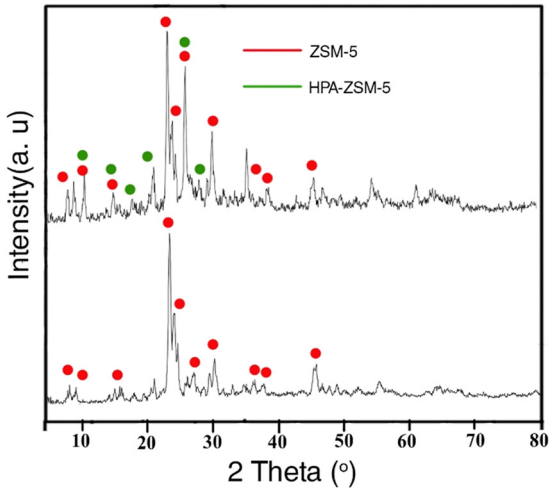

Figure 4: XRD of ZSM-5 and HPA-ZSM-5.

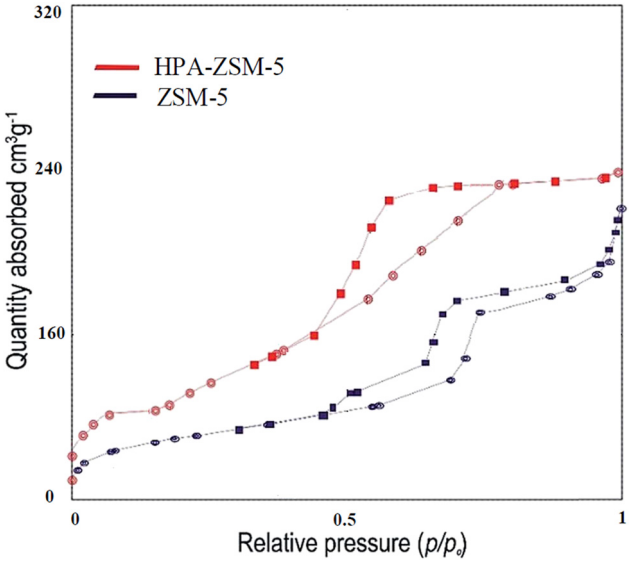

Figure 5: N_2 adsorption–desorption isotherms of ZSM-5 and HPA-ZSM-5.

solvent on the external surface and molecules trapped among HPA-ZSM-5. The curve indicated a weight loss of about 4.5% from 350°C to 550°C due to the decomposition of the phosphomolybdic acid grafting to ZSM-5.

We investigated the reaction of phenylhydrazine, benzaldehyde, and indan-1,2,3-trione as a model reaction. To obtain the ideal reaction conditions for the preparation of compound **4a**, we studied the diverse catalysts and solvents (Table 1). Screening of different catalysts containing Et_3N, PTSA, nano-ZrO_2, CAN, L-proline, nano-TiO_2, HPA, ZSM-5, and HPA-ZSM-5 revealed HPA-ZSM-5 (6 mg) as the most effective catalyst to perform this reaction at room temperature (Table 1). Seeking of the reaction scope demonstrated that various aromatic aldehydes can be utilized in this method (Table 2). These results showed that aromatic aldehydes with electron-withdrawing groups reacted faster than aldehydes with electron-releasing groups as expected.

The possibility of recycling the catalyst is an important process from different aspects such as environmental concerns and applicable commercial processes. The reusability of HPA-ZSM-5 was tested for the synthesis of **4a,** and it was found that product yields reduced to a small extent on each reuse (run 1, 92%, run 2, 92%, run 3, 92%, run 4, 91%, run 5, 91%, run 6, 90%). After completion of the reaction, HPA-ZSM-5 was separated from the mixture using filtration. HPA-ZSM-5 was rinsed five times with ethanol and dried at room temperature for 15 h.

A mechanism for the preparation of indenopyrazolones using HPA-ZSM-5 is proposed (Scheme 2). First, the activated benzaldehyde by HPA-ZSM-5 is condensed with phenylhydrazine to give intermediate I, which attacks indan-1,2,3-trione to afford the zwitterionic intermediate II. Its tautomer III undergoes an intramolecular

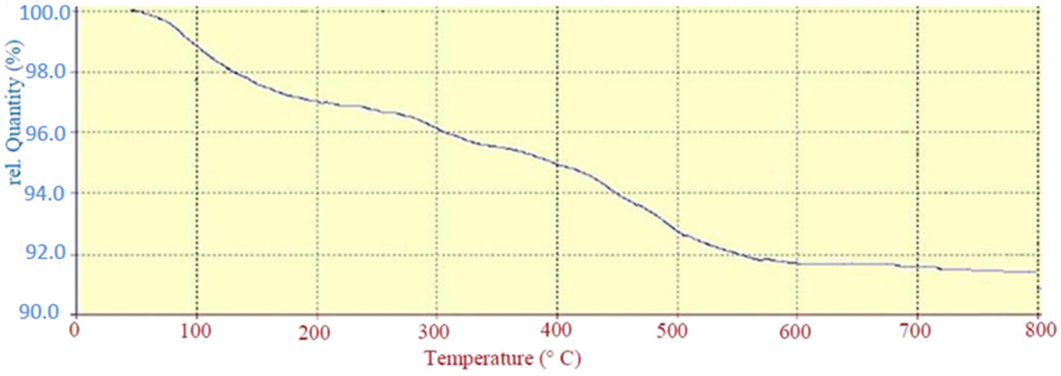

Figure 6: TGA curve of HPA-ZSM-5.

Table 1: Optimization of reaction conditions using different catalysts under different conditions[a]

Entry	Catalyst (amount)	Solvent	Time (min)	Yield (%)[b]
1	—	CH_3CN	300	17
2	Et_3N (5 mol%)	CH_3CN	200	22
3	L-Proline (5 mol%)	CH_3CN	150	25
4	CAN (4 mol%)	CH_3CN	150	31
5	*p*-TSA (4 mol%)	CH_3CN	150	40
6	Nano-ZrO_2(6 mg)	CH_3CN	140	48
7	Nano-TiO_2 (7 mg)	CH_3CN	140	42
8	HPA (4 mol%)	CH_3CN	80	60
9	ZSM-5 (8 mg)	CH_3CN	100	56
10	HPA-ZSM-5 (6 mg)	H_2O	60	60
11	HPA-ZSM-5 (6 mg)	DMF	50	73
12	HPA-ZSM-5 (6 mg)	EtOH	30	79
13	HPA-ZSM-5 (4 mg)	CH_3CN	30	84
14	HPA-ZSM-5 (6 mg)	CH_3CN	30	92
15	HPA-ZSM-5 (8 mg)	CH_3CN	30	92

[a]Phenylhydrazine (1 mmol), benzaldehyde (1 mmol), and indan-1,2,3-trione (1 mmol).
[b]Isolated yield.

nucleophilic addition reaction, which affords product by H-atom-transfer reaction. A highly regiospecific synthesis and crystal structure of indenopyrazolone was reported by Yavari et al. (2012). The *cis* configuration of the hydroxy groups was proven by nuclear magnetic resonance (NMR) (both –OH groups are involved in intramolecular H-bond and X-ray crystal) (Lobo et al., 2011; Pilipecz et al., 2007).

Table 2: Synthesis of indenopyrazolones

Entry	R	Product	Time (min)	Yield (%)[a]	m.p. (°C)
1	H	**4a**	30	92	221–223
2	4-OMe	**4b**	50	84	211–214
3	4-Me	**4c**	50	86	249–251
4	4-Cl	**4d**	25	94	234–236
5	4-Br	**4e**	25	94	222–224
6	4-NO_2	**4f**	25	95	242–244
7	3-NO_2	**4g**	30	92	240–243
8	4-OH	**4h**	60	82	202–204

[a]Isolated yield.

3 Conclusion

In conclusion, we demonstrated an effective method for the preparation of indenopyrazolones using HPA-ZSM-5 (6 mg) through a three-component reaction of phenylhydrazine, benzaldehydes and indan-1,2,3-trione at room temperature in acetonitrile. The zeolite catalyst has been characterized by XRD, FE-SEM, FT-IR, EDS, and N_2-adsorption analysis. Seeking of the reaction scope demonstrated that various aromatic aldehydes can be utilized in this method. These results showed that aromatic aldehydes with electron-withdrawing groups reacted faster than aldehydes with electron-releasing groups as expected. The advantages of this method include its great yields in concise times, the retrievable of the catalyst, low catalyst loading, and an easy work-up method.

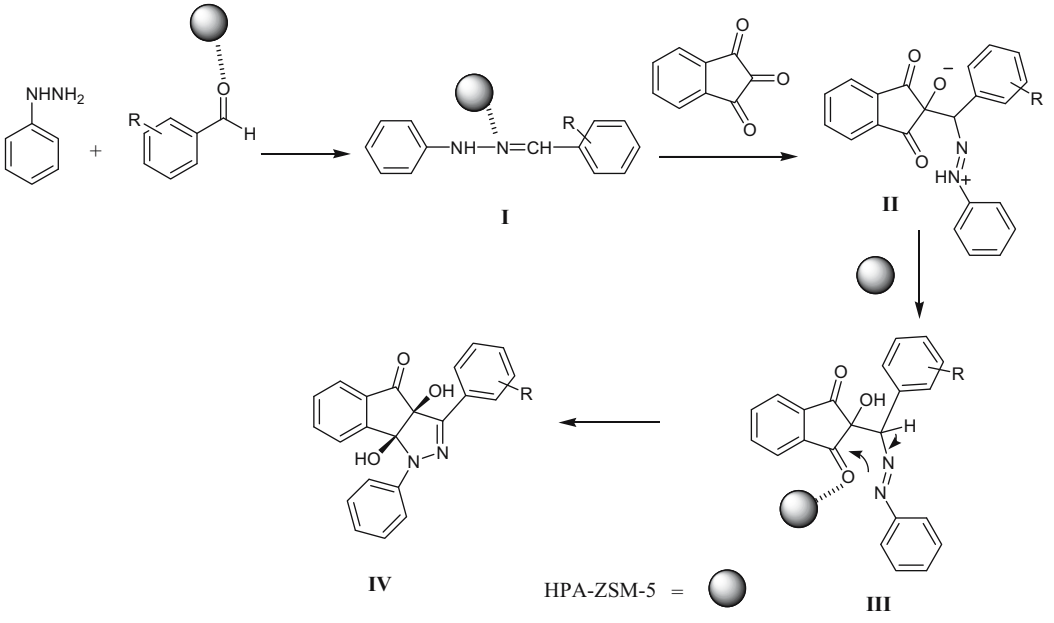

Scheme 2: Possible mechanism for the preparation of indenopyrazolones using HPA-ZSM-5.

Experimental

Chemicals and apparatus

NMR spectra were recorded on Bruker Avance-400 MHz spectrometers in the presence of tetramethylsilane as the internal standard. The infra red spectra were recorded on the FT-IR Magna 550 apparatus using KBr discs. Melting points were determined on Electrothermal 9200 and were not corrected. The elemental analyses (C, H, N) were obtained using a Carlo ERBA Model EA 1108 analyzer. The XRD patterns were recorded on an X-ray diffractometer (PHILIPS, PW 1510, Netherlands) using Cu-Kα radiation (λ = 0.154056 nm) in the range 2θ = 0.8–10°. FE-SEM of nanocatalyst was visualized by SEM (MIRA3). EDS measurement was carried out with the SAMX analyser. The N_2 adsorption/desorption analysis (BET) was performed using an automated gas adsorption analyser (BEL SORP mini II).

Preparation of ZSM-5

The zeolite precursor was prepared by adding tetrapropylammonium hydroxide, tetraethyl orthosilicate to a mixed aqueous solution of aluminium isopropoxide [Al(*i*Pro)$_3$], and NaOH with stirring. The mixture was converted to gel. The gel was stirred for 20 h. The mole composition of the gel was $1Al_2O_3$:$46SiO_2$:4TPA:$5Na_2O$:$2{,}500H_2O$. The resulting gel was sealed in Teflon-lined autoclaves and heated at 165°C for 72 h. The solid product was recovered by filtration, washed with deionized water several times, and dried in an oven at 100°C overnight. The as-synthesized material was then calcined at 550°C for 8 h to remove the templates.

Preparation of HPA-ZSM-5

ZSM-5 zeolites (1 g) were added to the solution of 0.3 g of phosphomolybdic acid (HPA) in ethanol (25 mL), and the reaction mixture was stirred for 24 h. The mixture was filtered, washed with deionized water several times, and dried in an oven at 100°C overnight. The as-synthesized material was subjected to product HPA-ZSM-5 at 400°C for 2 h.

General procedure for the synthesis of indenopyrazolones

A mixture of phenylhydrazine (1.0 mmol), benzaldehydes (1.0 mmol), ninhydrin (1.0 mmol) and 6 mg of HPA-ZSM-5 in acetonitrile (10 mL) was stirred for the appropriate times. After completion of the reaction thin layer chromatography , the catalyst was separated from the mixture using filtration. The solvent was evaporated, and the residue was washed with cold diethyl ether to get a pure product.

Spectra data

cis-3a,8b-Dihydro-3a,8b-dihydroxy-1,3-diphenylindeno[1,2-*c*]pyrazol-4(1*H*)-one (4a)

Yellow solid, m.p. 221–223°C, IR (KBr): ν_{max} = 3,433, 3,055, 1,736, 1,458 cm^{-1}. ^{1}H NMR (400 MHz, $CDCl_3$): δ (ppm) = 6.14 (s, OH), 6.19 (s, OH), 7.15 (d, J = 8.0 Hz, 1H, ArH), 7.19–7.31 (m, 3H, ArH), 7.42 (t, J = 7.6 Hz, 1H, ArH), 7.49 (t, J = 7.6 Hz, 1H, ArH), 7.53–7.67 (m, 5H, ArH), 8.23 (d, J = 7.6 Hz, 2H, ArH), 8.49 (d, J = 7.6 Hz, 1H, ArH). ^{13}C NMR (100 MHz, $CDCl_3$): δ (ppm) = 89.3 (C), 96.8 (C), 118.3 (2 CH), 121.5 (CH), 122.7 (CH), 123.3 (CH), 124.1 (CH), 126.3 (2 CH), 129.6 (2 CH), 130.8 (CH), 130.9 (C), 132.9 (2 CH), 133.6 (CH), 137.3 (C), 139.9 (C), 142.4 (C), 147.8 (C), 196.8 (C=O). Anal. calcd for $C_{22}H_{16}N_2O_3$: C, 74.15, H, 4.53, N, 7.86%, Found C, 74.12, H, 4.58, N, 7.93%.

cis-3a,8b-Dihydro-3a,8b-dihydroxy-3-(4-methoxyphenyl)-1-phenylindeno[1,2-*c*]pyrazol-4(1*H*)-one (4b)

Yellow solid, m.p. 211–214°C, IR (KBr): ν_{max} = 3,423, 3,284, 1,705, 1,593 cm^{-1}. ^{1}H NMR (400 MHz, $CDCl_3$): δ (ppm) = 3.66 (s, OCH_3), 6.14 (s, OH), 6.24 (s, OH), 6.89 (d, J = 8.2 Hz, 2H, ArH), 7.06 (t, J = 7.2 Hz, 1H, ArH), 7.19 (t, J = 7.4 Hz, 2H, ArH), 7.28 (t, J = 7.2 Hz, 1H, ArH), 7.39 (t, J = 7.4 Hz, 1H, ArH), 7.51 (d, J = 7.8 Hz, 1H, ArH), 7.56 (d, J = 7.4 Hz, 1H, ArH), 7.62 (d, J = 7.8 Hz, 2H, ArH), 8.03 (d, J = 8.4 Hz, 2H, ArH). ^{13}C NMR (100 MHz, $CDCl_3$): δ (ppm) = 55.5 (OCH_3), 90.2 (C), 96.5 (C), 113.6 (2 CH), 117.8 (2 CH), 122.4 (CH), 123.8 (CH), 124.4 (C), 125.9 (CH), 128.6 (2 CH), 129.4 (2 CH), 130.4 (CH), 135.4 (C), 136.8 (CH), 142.9 (C), 143.4 (C), 147.7 (C), 160.5 (C), 197.6 (C=O). Anal. calcd for $C_{23}H_{18}N_2O_4$: C, 71.49, H, 4.70, N, 7.25%, Found C, 71.39, H, 4.63, N, 7.19%.

cis-3a,8b-Dihydro-3a,8b-dihydroxy-3-(4-methylphenyl)-1-phenylindeno[1,2-*c*]pyrazol-4(1*H*)-one (4c)

Yellow solid, m.p. 249–251°C, IR (KBr): ν_{max} = 3,435, 3,266, 1,719, 1,588 cm^{-1}. ^{1}H NMR (400 MHz, $CDCl_3$): δ (ppm) = 2.34 (s, CH_3), 6.13 (s, OH), 6.16 (s, OH), 7.08

(t, J = 7.8 Hz, 1H, ArH), 7.21 (d, J = 7.9 Hz, 2H, ArH), 7.35 (t, J = 7.8 Hz, 2H, ArH), 7.52 (t, J = 7.8 Hz, 1H, ArH), 7.56 (t, J = 8.0 Hz, 1H, ArH), 7.72 (d, J = 7.9 Hz, 1H, ArH), 7.93 (d, J = 7.8 Hz, 2H, ArH), 8.08 (d, J = 7.7 Hz, 2H, ArH), 8.48 (d, J = 7.8 Hz, 1H, ArH). ^{13}C NMR (100 MHz, $CDCl_3$): δ (ppm) = 21.3 (CH_3), 89.5 (C), 95.6 (C), 126.1 (CH), 126.3 (2 CH), 126.7 (2 CH), 129.2 (CH), 129.5 (CH), 129.7 (2 CH), 129.8 (CH), 129.9 (2 CH), 130.8 (C), 134.6 (CH), 136.9 (C), 138.4 (C), 140.4 (C), 142.2 (C), 146.8 (C), 197.4 (C═O). Anal. calcd for $C_{23}H_{18}N_2O_3$: C, 74.58, H, 4.90, N, 7.56%, Found C, 74.48, H, 4.83, N, 7.53%.

cis-3-(4-Chlorophenyl)-3a,8b-dihydro-3a,8b-dihydroxy-1-phenylindeno[1,2-*c*]pyrazol-4(1*H*)-one (4d)

Yellow solid, m.p. 234–236°C, IR (KBr): ν_{max} = 3,452, 3,260, 1,699, 1,593 cm^{-1}. ^{1}H NMR (400 MHz, $CDCl_3$): δ (ppm) = 6.08 (s, OH), 6.12 (s, OH), 7.03 (t, J = 7.8 Hz, 1H, ArH), 7.33 (t, J = 7.8 Hz, 2H, ArH), 7.41–7.51 (m, 3H, ArH), 7.53 (t, J = 7.8 Hz, 1H, ArH), 7.63 (d, J = 7.3 Hz, 1H, ArH), 7.74 (d, J = 7.0 Hz, 1H, ArH), 7.86 (d, J = 7.1 Hz, 2H, ArH), 8.15 (d, J = 7.7 Hz, 2H, ArH). ^{13}C NMR (100 MHz, $CDCl_3$): δ (ppm) = 89.7 (C), 96.7 (C), 118.2 (2 CH), 122.6 (CH), 124.5 (CH), 126.3 (CH), 128.6 (2 CH), 128.9 (2 CH), 129.4 (2 CH), 130.3 (C), 130.9 (CH), 134.9 (C), 135.6 (C), 136.8 (CH), 142.7 (C), 142.9 (C), 147.6 (C), 197.3 (C═O). Anal. calcd for $C_{22}H_{15}ClN_2O_3$: C, 67.61, H, 3.87, N, 7.17%, Found C, 67.54, H, 3.84, N, 7.13%.

cis-3-(4-Bromophenyl)-3a,8b-dihydro-3a,8b-dihydroxy-1-phenylindeno[1,2-*c*]pyrazol-4(1*H*)-one (4e)

Yellow solid, m.p. 222–224°C, IR (KBr): ν_{max} = 3,440, 3,255, 1,694, 1,585 cm^{-1}. ^{1}H NMR (400 MHz, $CDCl_3$): δ (ppm) = 6.03 (s, OH), 6.15 (s, OH), 7.07 (t, J = 7.8 Hz, 1H, ArH), 7.39 (t, J = 7.3 Hz, 2H, ArH), 7.51 (t, J = 7.9 Hz, 1H, ArH), 7.62 (d, J = 7.9 Hz, 2H, ArH), 7.72 (t, J = 7.1 Hz, 1H, ArH), 7.82 (d, J = 7.6 Hz, 1H, ArH), 7.91–7.99 (m, 3H, ArH), 8.06 (d, J = 7.9 Hz, 2H, ArH). ^{13}C NMR (100 MHz, $CDCl_3$): δ (ppm) = 89.6 (C), 96.4 (C), 118.4 (2 CH), 122.9 (CH), 124.4 (CH), 126.3 (CH), 128.7 (2 CH), 129.3 (2 CH), 130.5 (C), 130.6 (CH), 131.7 (2 CH), 135.5 (C), 136.8 (CH), 137.2 (C), 142.3 (C),142.7 (C), 147.6 (C), 196.4 (C═O). Anal. calcd for $C_{22}H_{15}BrN_2O_3$: C, 60.71, H, 3.47, N, 6.44%, Found C, 60.64, H, 3.42, N, 6.33%.

cis-3a,8b-Dihydro-3a,8b-dihydroxy-3-(4-nitrophenyl)-1-phenylindeno[1,2-*c*]pyrazol-4(1*H*)-one (4f)

Yellow solid, m.p. 242–244°C, IR (KBr): ν_{max} = 3,401, 3,042, 1,718, 1,562, 1,353 cm^{-1}. ^{1}H NMR (400 MHz, $CDCl_3$): δ (ppm) = 6.09 (s, OH), 6.17 (s, OH), 7.15–7.26 (m, 5H, ArH), 7.29–7.61 (m, 4H, ArH), 8.26 (d, J = 7.1 Hz, 2H, ArH), 8.38 (d, J = 7.2 Hz, 2H, ArH). ^{13}C NMR (100 MHz, $CDCl_3$): δ (ppm) = 89.6 (C), 97.8 (C), 118.4 (2 CH), 122.6 (2 CH), 123.3 (CH), 123.4 (CH), 125.5 (CH), 126.8 (2 CH), 128.9 (2 CH), 130.5 (CH), 134.6 (C), 136.5 (CH), 137.9 (C), 140.7 (C), 142.3 (C), 146.9 (C), 147.5 (C), 197.3 (C═O). Anal. calcd for $C_{22}H_{15}N_3O_5$: C, 65.83, H, 3.77, N, 10.47%, Found C, 65.74, H, 3.72, N, 10.43%.

cis-3a,8b-Dihydro-3a,8b-dihydroxy-3-(3-nitrophenyl)-1-phenylindeno[1,2-*c*]pyrazol-4(1*H*)-one (4g)

Yellow solid, m.p. 240–242°C, IR (KBr): ν_{max} = 3,463, 1,725, 1,591, 1,504 cm^{-1}. ^{1}H NMR (400 MHz, $CDCl_3$): δ (ppm) = 6.26 (s, OH), 6.37 (s, OH), 7.51–7.81 (m, 10H, ArH), 8.08 (d, J = 8.1 Hz, 1H, ArH), 8.52 (d, J = 7.8 Hz, 1H, ArH), 8.62 (s, 1H, ArH). ^{13}C NMR (100 MHz, $CDCl_3$): δ (ppm) = 89.4 (C), 96.8 (C), 118.3 (2 CH), 121.6 (CH), 122.8 (CH), 123.3 (CH), 124.1 (CH), 126.3 (CH), 129.6 (2 CH), 129.7 (CH), 130.8 (CH), 132.9 (CH), 133.4 (C), 135.3 (C), 137.2 (CH), 140.9 (C), 142.8 (C), 147.7 (C), 147.4 (C), 196.8 (C═O). Anal. calcd for $C_{22}H_{15}N_3O_5$: C, 65.83, H, 3.77, N, 10.47%, Found C, 65.73, H, 3.69, N, 10.36%.

cis-3a,8b-Dihydro-3a,8b-dihydroxy-3-(4-hydroxyphenyl)-1-phenylindeno[1,2-*c*]pyrazol-4(1H)-one (4h)

Yellow solid, m.p. 202–204°C, IR (KBr): ν_{max} = 3,421, 1,756, 1,535, 1,457 cm^{-1}. ^{1}H NMR (400 MHz, $CDCl_3$): δ (ppm) = 4.59 (s, OH), 6.14 (s, OH), 6.18 (s, OH), 6.96 (t, J = 7.4 Hz, 2H, ArH), 7.16–7.23 (m, 2H, ArH), 7.27 (m, 1H, ArH), 7.41–7.51 (m, 2H, ArH), 7.56–7.62 (m, 5H, ArH), 7.94 (d, J = 7.8 Hz, 1H, ArH). ^{13}C NMR (100 MHz, $CDCl_3$): δ (ppm) = 89.3 (C), 94.1 (C), 116.4 (CH), 118.5 (2 CH), 119.3 (CH), 123.9 (CH), 124.5 (CH), 125.6 (CH), 127.8 (CH), 129.4 (2 CH), 134.6 (C), 134.8 (C), 137.3 (CH), 141.2 (C), 144.9 (C), 146.3 (C), 157.5 (C), 197.3 (C═O). Anal. calcd for $C_{22}H_{16}N_2O_4$: C, 70.96, H, 4.33, N, 7.52%, Found C, 70.83, H, 4.25, N, 7.43%.

Acknowledgments: The authors acknowledge a reviewer who provided helpful insights. The authors are grateful to University of Kashan for supporting this work by Grant no: 159196/XXI.

Funding information: The researchers are thankful to the University of Kashan for supporting this work through Grant No. 363010/III.

Author contributions: Seyyed Mohammad Ebrahimi: experimental data collection, writing; Javad Safaei-Ghomi: project resources and supervision; Mohammaed Abdulridha Mutashar: project administration, writing.

Conflict of interest: Authors state no conflict of interest.

References

Ahsan M.J., Khalilullah H., Stables J.P., Govindasamy J., Synthesis and anticonvulsant activity of 3a,4-dihydro-3H-indeno[1,2-*c*] pyrazole-2-carboxamide/carbothioamide analogues. J. Enzyme Inhib. Med Chem., 2013, 28, 644–650.

Akondi A.M., Kantam M.L., Trivedi R., Bharatam J., Vemulapalli S.P.B., Bhargava S.K., et al., Ce/SiO_2 composite as an efficient catalyst for the multicomponent one-pot synthesis of substituted pyrazolones in aqueous media and their antimicrobial activities. J. Mol. Catal. A. Chem., 2016, 411, 325–336.

Alirezvani, Z., Dekamin M.G., Valiey E., Cu(II) and magnetite nanoparticles decorated melamine-functionalized chitosan: A synergistic multifunctional catalyst for sustainable cascade oxidation of benzyl alcohols/Knoevenagel condensation. Sci. Rep. 2019, 9, 17758–17769.

Amini M.M., Shaabani A., Bazgir A., Tangstophosphoric acid ($H_3PW_{12}O_{40}$): An efficient and eco-friendly catalyst for the one-pot synthesis of dihydropyrimidin-2 (1H)-ones. Catal. Commun., 2006, 7, 843–847.

Bordoloi A., Lefebvre F., Halligudi S.B., Selective oxidation of anthracene using inorganic–organic hybrid materials based on molybdovanadophosphoric acids. J. Catal. 2007, 247, 166–175.

Davoodi F., Dekamin M.G., Alirezvani Z., A practical and highly efficient synthesis of densely functionalized nicotinonitrile derivatives catalyzed by zinc oxide-decorated superparamagnetic silica attached to graphene oxide nanocomposite. Appl. Organometal. Chem. 2019, 33, 4735-4747.

Dai F., Luo J., Zhou S., Qin X., Liu D., Qi H., Porous hafnium-containing acid/base bifunctional catalysts for efficient upgrading of bio-derived aldehydes. J. Bioresour. Bioprod. 2021, 6, 243–253.

Ghanbari D., Sharifi S., Naraghi A., Nabiyouni G., Photo-degradation of azo-dyes by applicable magnetic zeolite Y–Silver–$CoFe_2O_4$ nanocomposites. J. Mater. Sci.: Mater. Electron., 2016, 27, 5315–5323.

Gholamian F., Salavati-Niasari M., Ghanbari D., Sabet M., The effect of flower-like magnesium hydroxide nanostructure on the thermal stability of cellulose acetate and acrylonitrile–butadiene–styrene. J. Clust. Sci., 2013, 24, 73–84.

Indrasena A., Riyaz S., Mallipeddi P.L., Padmaja P., Sridhar B., Dubey P.K., Design, synthesis, and biological evaluation of indolylidinepyrazolones as potential anti-bacterial agents. Tetrahedron Lett., 2014, 55, 5014–5018.

Izumi Y., Hisano K., Hida T., Acid catalysis of silica-included heteropolyacid in polar reaction media. Appl. Catal. A: Gen., 1999, 181, 277–282.

Javidi J., Esmaeilpour M., Rahiminezhad Z., Dodeji F.N., Synthesis and characterization of H3PW12O40 and H3PMo12O40 nanoparticles by a simple method. J. Clust. Sci., 2014, 25, 1511–1524.

Karimi-Maleh H., Karimi F., Orooji Y., Mansouri G., Razmjou A., Aygun A., et al., A new nickel-based co-crystal complex electrocatalyst amplified by NiO dope Pt nanostructure hybrid; a highly sensitive approach for determination of cysteamine in the presence of serotonin. Sci. Rep., 2020, 10, 11699–11712.

Kaur N., Kumar A., Singh K., Synthesis of Novel Indenopyrimidine Sulfonamides from Indenopyrimidine-2-Amines via S–N Bond Formation. Polycycl. Aromat. Compd., 2020. doi: 10.1080/10406638.2020.1809470.

Keyikoglu R., Khataee A., Lin H., Orooji Y., Vanadium (V)-doped ZnFe layered double hydroxide for enhanced sonocatalytic degradation of pymetrozine. Biochem. Eng. J., 2022, 434, 134730–134739.

Khalil N.A., Ahmed E.M., Mohamed K.O., Nissan Y.M., Zaitone S.A.B., Synthesis and biological evaluation of new pyrazolone–pyridazine conjugates as anti-inflammatory and analgesic agents. Bioorg. Med. Chem., 2014, 22, 2080–2089.

Liu P., Zhang Z., Jia M., Gao X., Yu J., ZSM-5 zeolites with different SiO_2/Al_2O_3 ratios as fluid catalytic cracking catalyst additives for residue cracking. Chin. J. Catal., 2015, 36, 806–812.

Lobo G., Zuleta E., Charris K., Capparelli M.V., Briceno A., Angel J., et al., Synthesis and crystal structure of (4bRS,9bRS)-5-(2,4-dimethoxyphenyl)-4b,9b-7,7-dimethyldihydroxy-4b,5,6,7,8,9b-hexahydroindeno[1,2-b]indole-9,10-dione. J. Chem. Res., 2011, 35, 222–224.

Masoumi S., Nabiyouni G., Ghanbari D., Photo-degradation of Congored, acid brown and acid violet: photo catalyst and magnetic investigation of $CuFe_2O_4$–TiO_2–Ag nanocomposites. J. Mater. Sci.: Mater. Electron., 2016, 27, 11017–11033.

Mazimba O., Wale K., Loeto D., Kwape T., Antioxidant and antimicrobial studies on fused-ring pyrazolones and isoxazolones. Bioorg. Med. Chem., 2014, 22, 6564–6569.

Molnár A., Keresszegi C., Török B., Heteropoly acids immobilized into a silica matrix: characterization and catalytic applications. Appl. Catal. A: Gen., 1999, 189, 217–224.

Mor S., Mohil R., Nagoria S., Kumar A., Lal K., Kumar D., et al., Regioselective Synthesis, Antimicrobial Evaluation and QSAR Studies of Some 3-Aryl-1-heteroarylindeno[1,2-*c*]pyrazol-4(1H)-ones. J. Heterocycl. Chem., 2017, 54, 1327–1341.

Mor S., Sindhu S., Synthesis, type II diabetes inhibitory activity, antimicrobial evaluation and docking studies of indeno[1,2-*c*] pyrazol-4(1H)-ones. Med. Chem. Res., 2020, 29, 46–62.

Mor S., Sindhu S., Nagoria S., Khatri M., Garg P., Sandhu H., et al., Synthesis, biological evaluation, and molecular docking studies of some N-thiazolyl hydrazones and indenopyrazolones. J. Heterocycl. Chem., 2019, 56, 1622–1633.

Mukai S.R., Shimoda M., Lin L., Tamon H., Masuda T., Improvement of the preparation method of “ship-in-the-bottle” type 12-

molybdophosphoric acid encaged Y-type zeolite catalysts. Appl. Catal. A: Gen., 2003, 256, 107–113.

Nabiyouni G., Ghanbari D., Ghasemi J., Yousofnejad A., Microwave-assisted synthesis of $MgFe_2O_4$-ZnO nanocomposite and its photo-catalyst investigation in methyl orange degradation. J. Nanostruct., 2015, 5, 289–295.

Niknam K., Saberi D., Sadegheyan M., Deris A., Silica-bonded S-sulfonic acid: an efficient and recyclable solid acid catalyst for the synthesis of 4, 4′-(arylmethylene) bis (1H-pyrazol-5-ols). Tetrahedron Lett., 2010, 51, 692–694.

Orooji Y., Tanhaei B., Ayati A., Tabrizi S.H., Alizadeh M., Bamoharram F.F., et al., Heterogeneous UV-Switchable Au nanoparticles decorated tungstophosphoric acid/TiO_2 for efficient photocatalytic degradation process. Chemosphere., 2021, 281, 130795–130804.

Pilipecz M.V., Mucsi Z., Nemes P., Scheiber P., Chemistry of nitroenamines. synthesis of pyrrolizine derivatives. Heterocycles 2007, 71, 1919–1928.

Rostom S.A.F., Synthesis and in vitro antitumor evaluation of some indeno[1,2-*c*]-pyrazol(in)es substituted with sulfonamide, sulfonylurea(-thiourea)pharmacophores, and some derived thiazole ring systems. Bioorg. Med. Chem., 2006, 14, 6475–6485.

Safaei-Ghomi J., Abbas A.K., Shahpiri M., Synthesis of imidazoles promoted by $H_3PW_{12}O_{40}$-amino-functionalized $CdFe_{12}O_{19}$@SiO_2 nanocomposite. Nanocomposites, 2020, 6, 149–157.

Saidachary G., Veera Prasad K., Divya D., Singh A., Ramesh U., Sridhar B., et al., Convenient one-pot synthesis, anti-mycobacterial and anticancer activities of novel benzoxepinoisoxazolones and pyrazolones. Eur. J. Med. Chem., 2014, 76, 460–469.

Sivakumar K.K., Rajasekaran A., Senthilkumar P., Wattamwar P.P., Conventional and microwave assisted synthesis of pyrazolone Mannich bases possessing anti-inflammatory, analgesic, ulcerogenic effect and antimicrobial properties. Bioorg. Med. Chem. Lett., 2014, 24, 2940–2944.

Singh K., Sharma P.K., Dhawan S.N., Singh S.P., Synthesis and characterisation of some novel indeno[1,2-*c*]pyrazoles. J. Chem. Research., 2005, 2005, 526–529.

Singh K., Applications of indan-1,3-dione in heterocyclic synthesis. Curr. Org. Synth., 2016, 13, 385–407.

Sobhani S., Hasaninejad A.R., Maleki M.F., Parizi Z.P., Tandem Knoevenagel–Michael reaction of 1-Phenyl-3-methyl-5-pyrazolone with Aldehydes using 3-aminopropylated silica gel as an efficient and reusable heterogeneous catalyst. Synth. Commun., 2012, 42, 2245–2255.

Sofia L.T.A., Krishnan A., Sankar M., Raj N.K.K., Manikandan P., Rajamohanan P.R., et al., Immobilization of phosphotungstic acid (pta) on imidazole functionalized silica: evidence for the nature of pta binding by solid state nmr and reaction studies. J. Phys. Chem. C., 2009, 113, 21114–21122.

Su M., Li W., Ma Q., Zhu B., Production of jet fuel intermediates from biomass platform compounds via aldol condensation reaction over iron-modified MCM-41 lewis acid zeolite. J. Bioresour.Bioprod., 2020, 5, 256–265.

Sunita G., Devassy B.M., Vinu A., Sawant D.P., Balasubramanian V.V., Halligudi S.B., Synthesis of biodiesel over zirconia-supported isopoly and heteropoly tungstate catalysts. Catal. Commun., 2008, 9, 696–702.

Taherian Z., Gharahshiran V.S., Khataee A., Orooji Y., Synergistic effect of freeze-drying and promoters on the catalytic performance of Ni/MgAl layered double hydroxide. Fuel., 2022, 311, 122620–122629.

Takmil N.F., Jaleh B., Mohazzab B.F., Khazalpour S., Rostami-Vartooni A., Nguyen T.H.C., et al., Hydrogen production by Electrochemical reaction using waste zeolite boosted with Titania and Au nanoparticles. Inorg. Chem. Commun., 2021, 133, 108891–108896.

Timofeeva M.N., Acid catalysis by heteropoly acids. Appl. Catal. A: Gen. 2003, 256, 19–35.

Waghmare N.G., Kasinathan P., Amrute A., Lucas N., Halligudi S.B., Titania supported silicotungstic acid: An efficient solid acid catalyst for veratrole acylation. Catal. Commun. 2008, 9, 2026–2029.

Wang W., Wang S.X., Qin X.Y., Li J.T., Reaction of aldehydes and pyrazolones in the presence of sodium dodecyl sulfate in aqueous media. Synth. Commun., 2005, 35, 1263–1269.

Wang J., Zhu H., Alkylation of 1-dodecene with benzene over $H_3PW_{12}O_{40}$ supported on mesoporous silica SBA-15. Catal. Lett., 2004, 93, 209–212.

Xue Z., Ma J., Zhang T., Miao H., Li R., Synthesis of nanosized ZSM-5 zeolite with intracrystalline mesopores. Mater. Lett., 2012, 68, 1–3.

Yavari I., Seyfi S., Skoulika S., A convenient synthesis of functionalized indenopyrazolones from indan-1, 2, 3-trione, benzaldehydes, and phenylhydrazine. Helvetica Chimica Acta., 2012, 95, 1581–1585.

Zang H., Su Q., Mo Y., Cheng B., Ionic liquid under ultrasonic irradiation towards a facile synthesis of pyrazolone derivatives. Ultrason. Sonochem., 2011, 18, 68–72.

Appendix

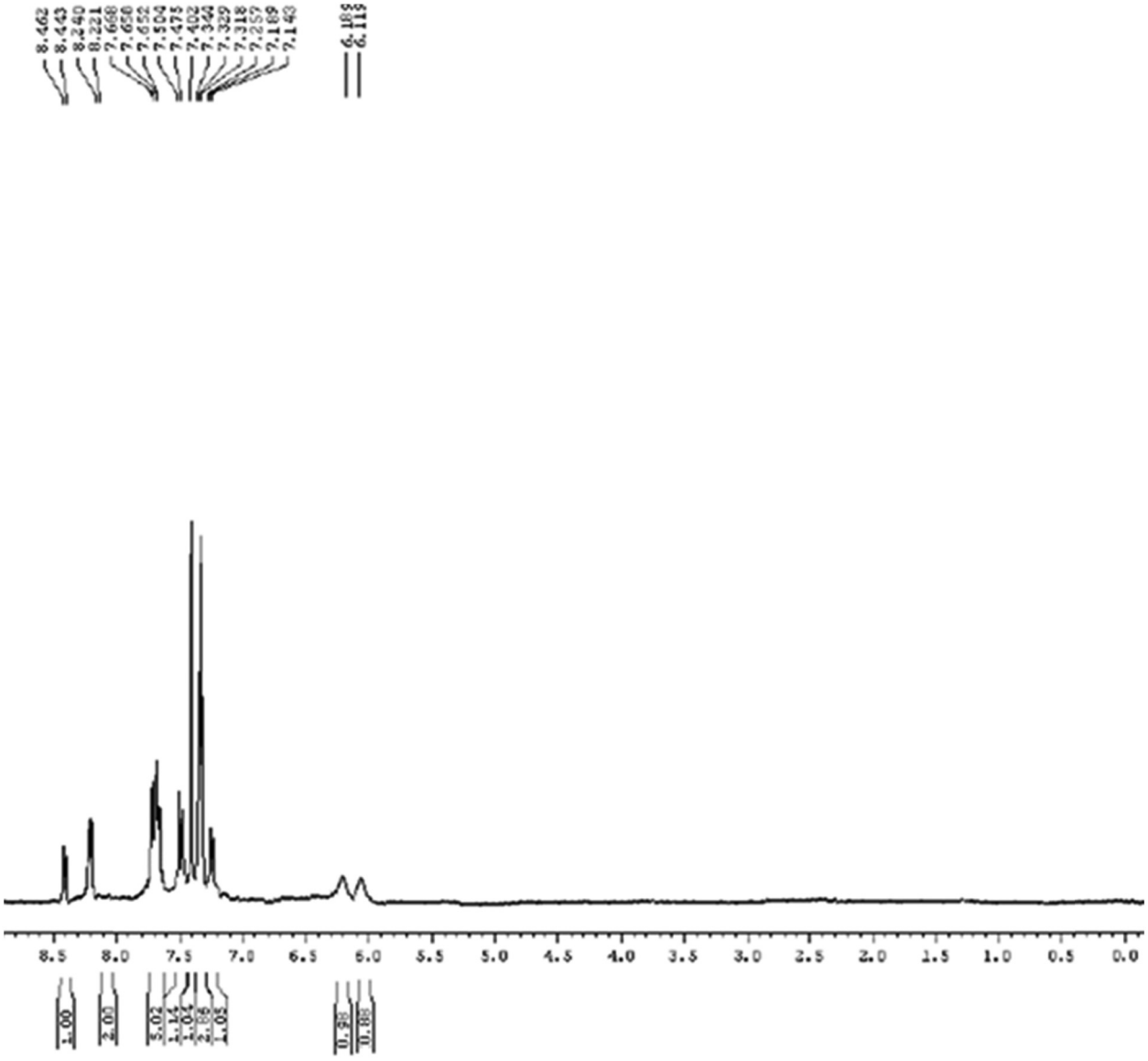

Figure A1: *cis*-3a,8b-Dihydro-3a,8b-dihydroxy-1,3-diphenylindeno[1,2-*c*]pyrazol-4(1*H*)-one (**4a**).

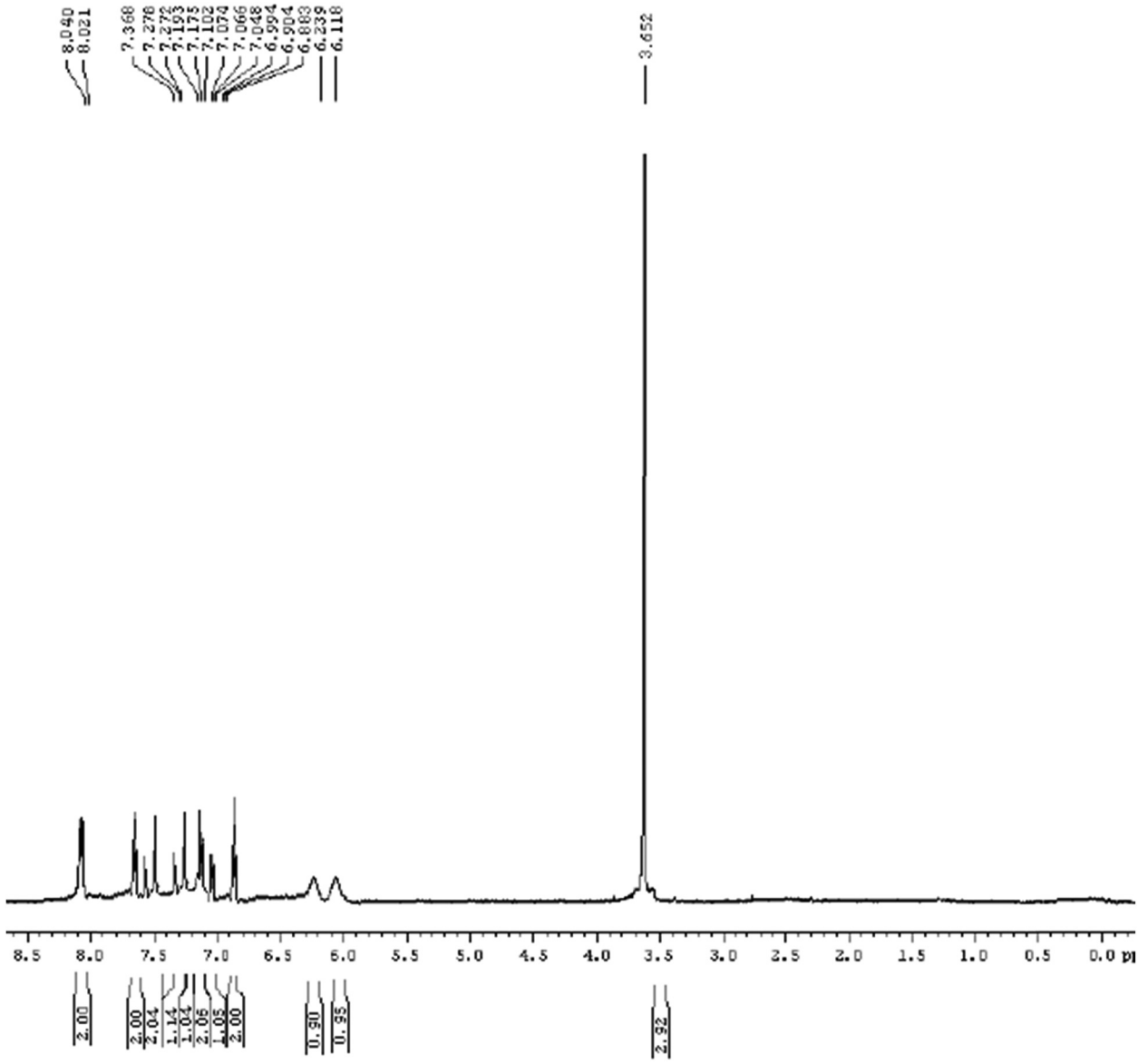

Figure A2: *cis*-3a,8b-Dihydro-3a,8b-dihydroxy-3-(4-methoxyphenyl)-1-phenylindeno[1,2-*c*]pyrazol-4(1*H*)-one (**4b**).

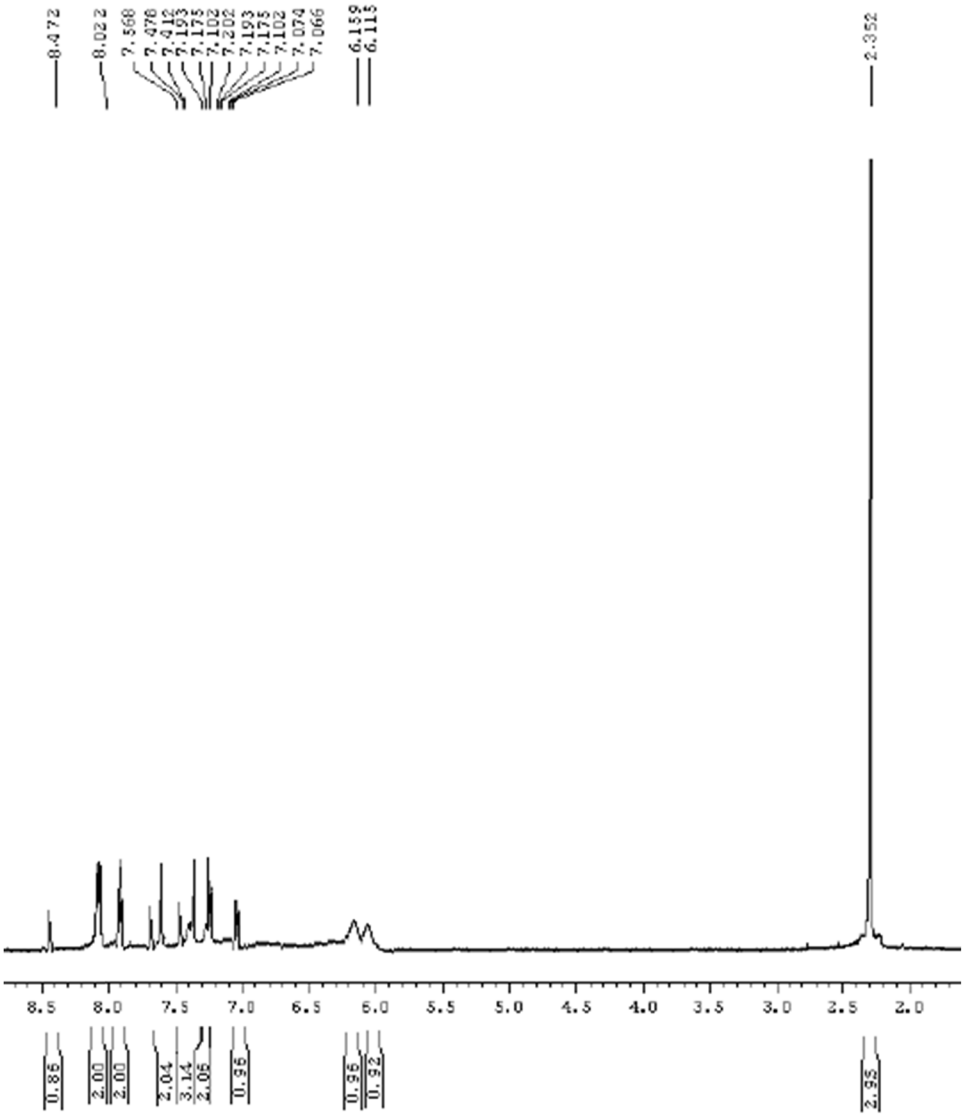

Figure A3: *cis*-3a,8b-Dihydro-3a,8b-dihydroxy-3-(4-methylphenyl)-1-phenylindeno[1,2-*c*]pyrazol-4(1*H*)-one (**4c**).

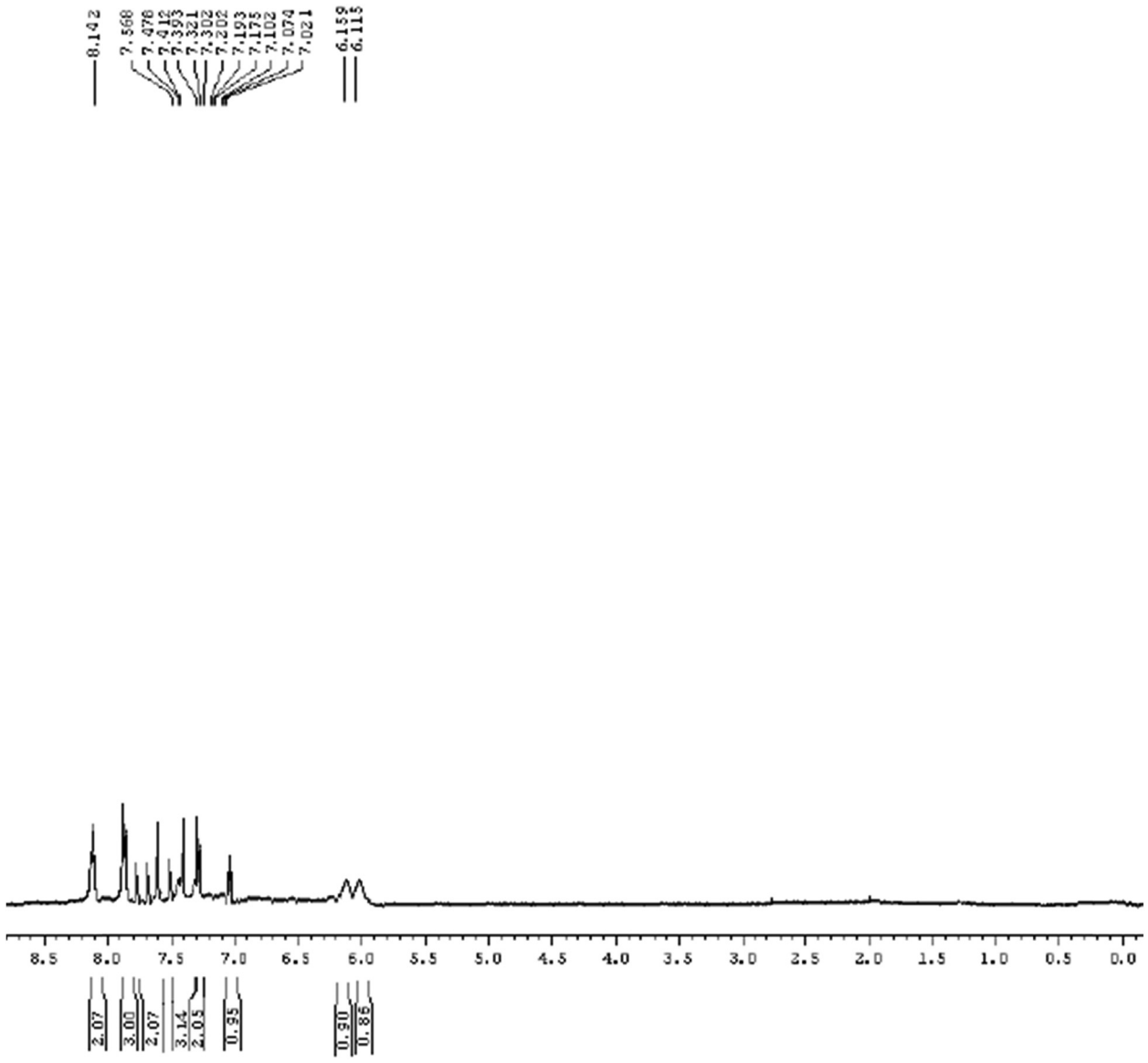

Figure A4: *cis*-3-(4-Chlorophenyl)-3a,8b-dihydro-3a,8b-dihydroxy-1-phenylindeno[1,2-*c*]pyrazol-4(1*H*)-one (**4d**).

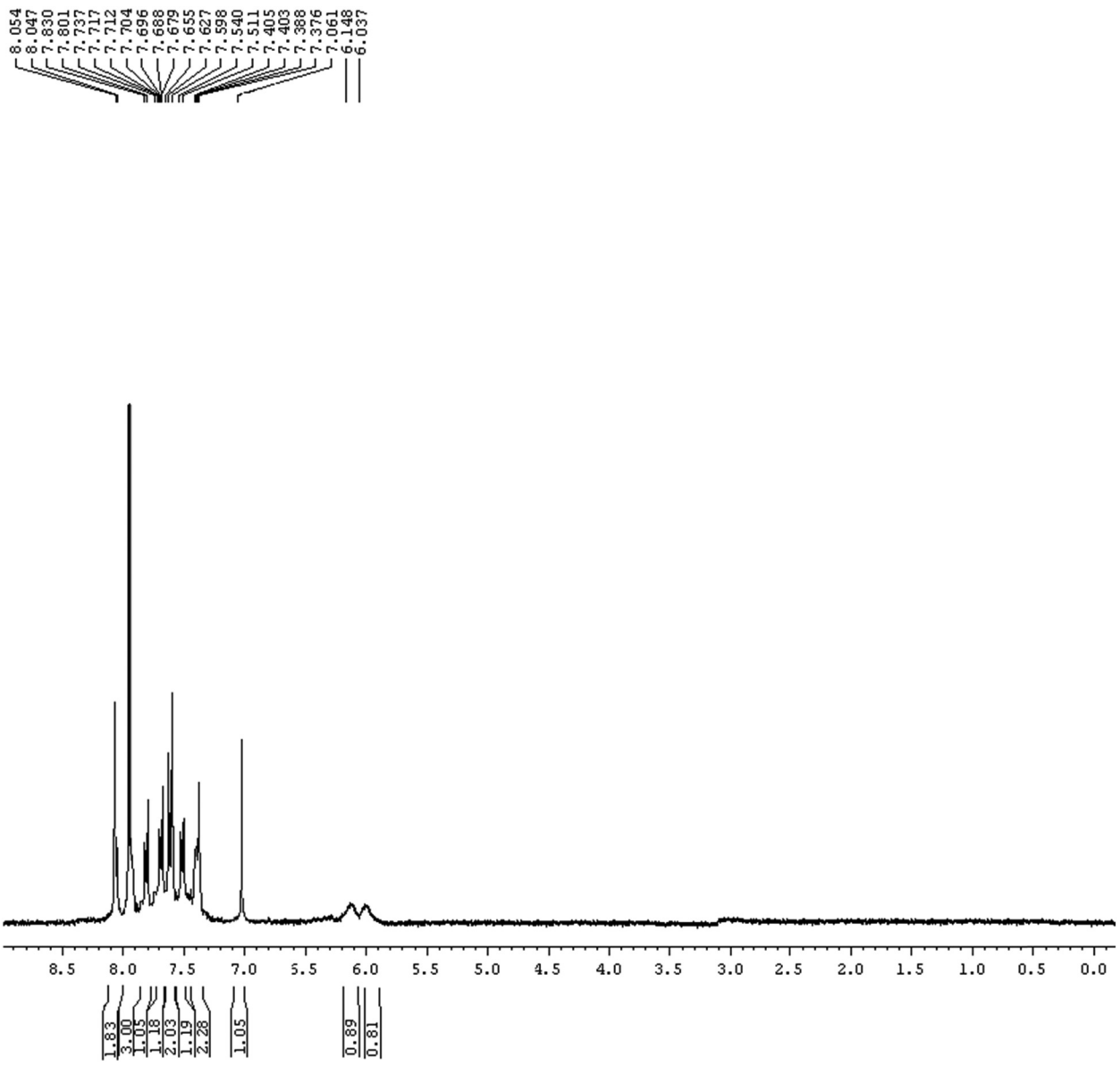

Figure A5: *cis*-3-(4-Bromophenyl)-3a,8b-dihydro-3a,8b-dihydroxy-1-phenylindeno[1,2-*c*]pyrazol-4(1*H*)-one (**4e**).

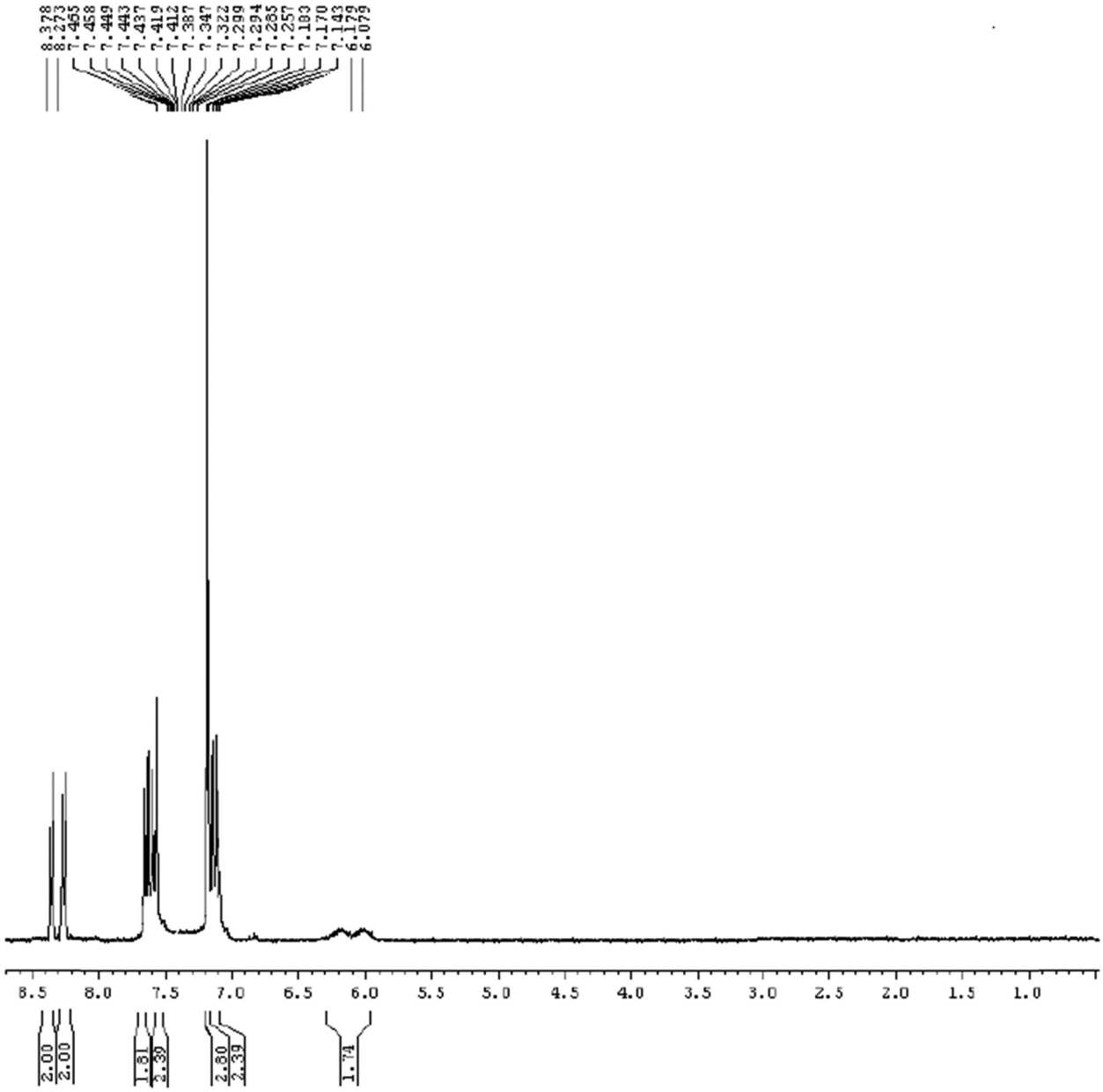

Figure A6: *cis*-3a,8b-Dihydro-3a,8b-dihydroxy-3-(4-nitrophenyl)-1-phenylindeno[1,2-*c*]pyrazol-4(1*H*)-one (**4f**).

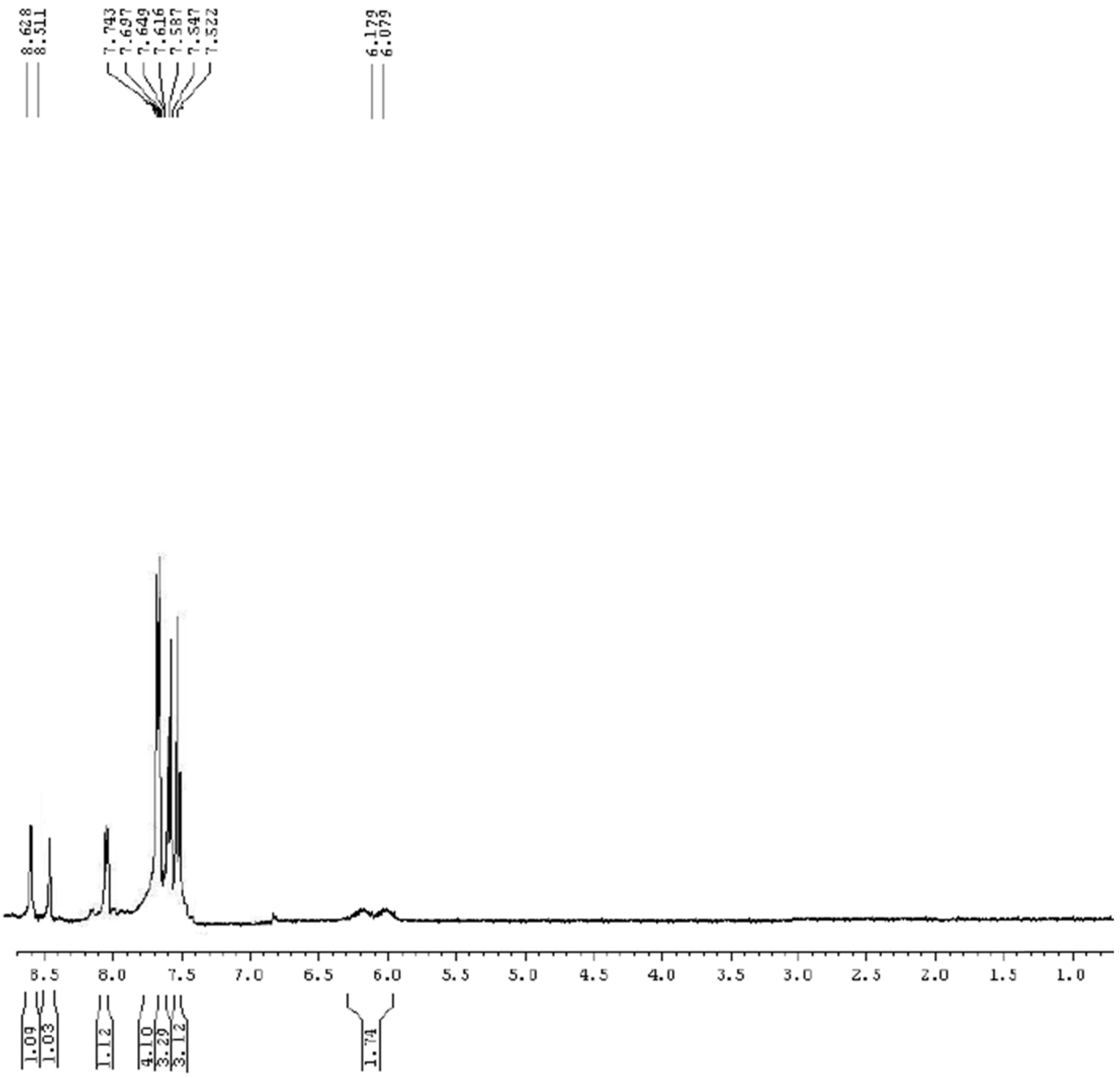

Figure A7: *cis*-3a,8b-Dihydro-3a,8b-dihydroxy-3-(3-nitrophenyl)-1-phenylindeno[1,2-*c*]pyrazol-4(1*H*)-one (**4g**).

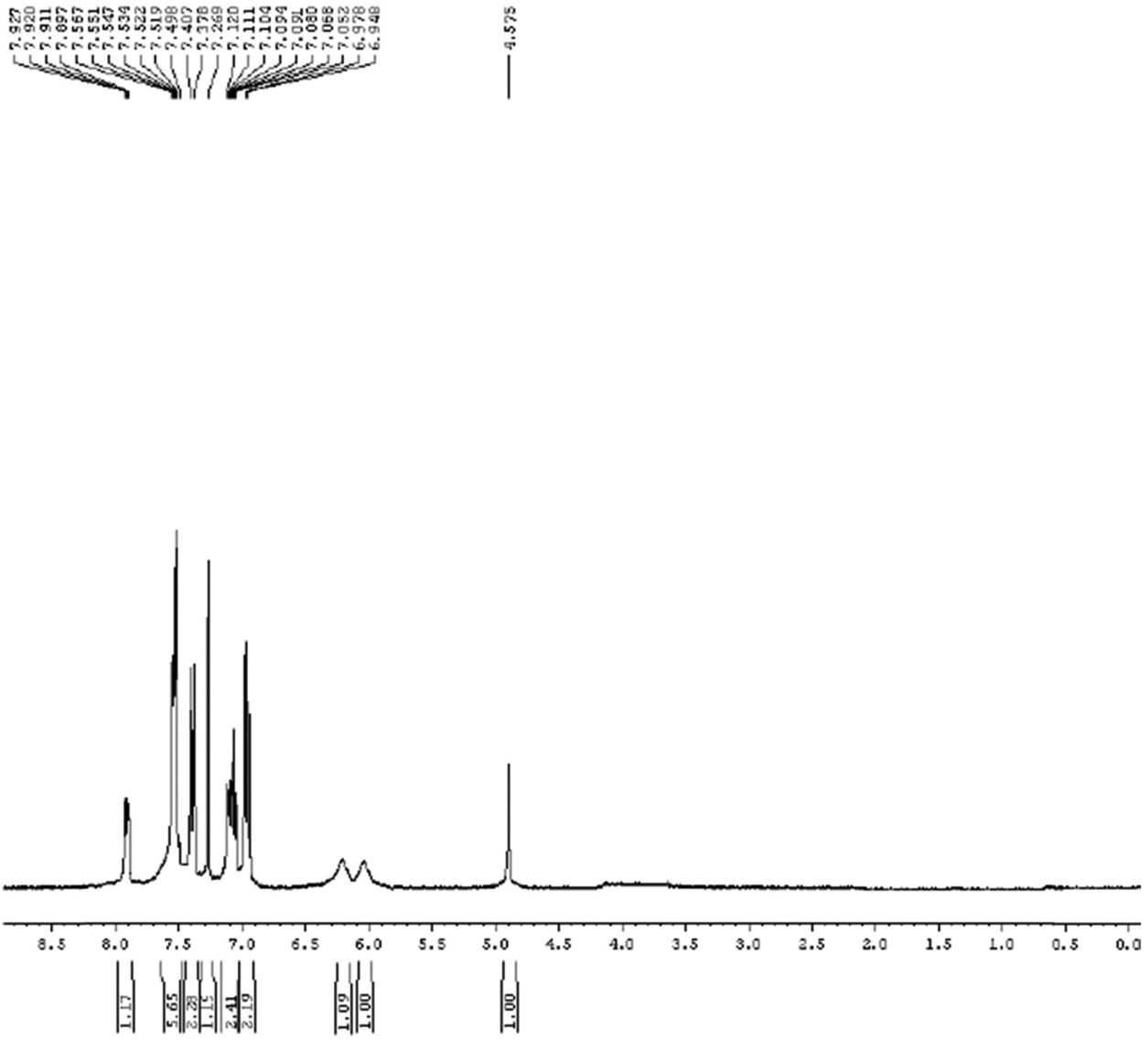

Figure A8: *cis*-3a,8b-Dihydro-3a,8b-dihydroxy-3-(4-hydroxyphenyl)-1-phenylindeno[1,2-*c*]pyrazol-4(1*H*)-one (**4h**).